Next-generation all-solid-state battery (#ASSB)

Tuan Vo[a,b †], Claas Hüter[b], Stefanie Braun[a], Manuel Torrilhon[a]

[a]Department of Mathematics, Applied and Computational Mathematics (ACoM), RWTH Aachen University, Schinkelstraße 02, 52062 Aachen, Germany
[b]Institute of Energy and Climate Research (IEK-2), Forschungszentrum Jülich, Wilhelm-Johnen-Straße, 52428 Jülich, Germany

Mathematical modelling for the next-generation All-solid-state batteries: Nucleation (SE|SSE)$^{(*)}$-interface

Rechargeable Lithium-ion battery (LIB) is at the heart of every electric vehicle (EV), portable electronic device, and energy storage system [1]. Nowadays, LIBs enable human life more efficient and help to solve global environment issues thanks to EVs' zero emission. However, conventional LIB (c-LIB) is sensible to temperature and pressure, hence, flammable and explosive, which is undesirable. This bottleneck is mainly due to liquid-based electrolyte found in c-LIBs.

All-solid-state battery (ASSB) is one of promising candidates to overcome bottlenecks of c-LIBs. Thanks to solid-state electrolyte (SSE), ASSB is highly stable towards temperature and pressure. Nevertheless, Li-metal dendrite triggered at (SE|SSE)-interface is the main drawback of ASSB since these dendritic threads extrapolate into SSE grain boundary network, causing crevice, degradation of ionic conductivity, and the probability of short-circuit, which is unfavorable.

Next-generation All-solid-state battery (ng-ASSB) with a consideration of nucleation criterion defined by

$$a_{\text{Griffith}} := a^* = \arg\min_{a\in\mathbb{R}} \iiint_\Omega f(a, \boldsymbol{u}; \lambda, \mu, \boldsymbol{d}\otimes\boldsymbol{d})\, d\Omega - \iint_\Gamma f(a;\gamma)\, d\Gamma \Big|_{\boldsymbol{u}^{(s)}}$$

where, can help to improve ASSB performance.
can help to improve ASSB performance.
can help to improve ASSB performance.

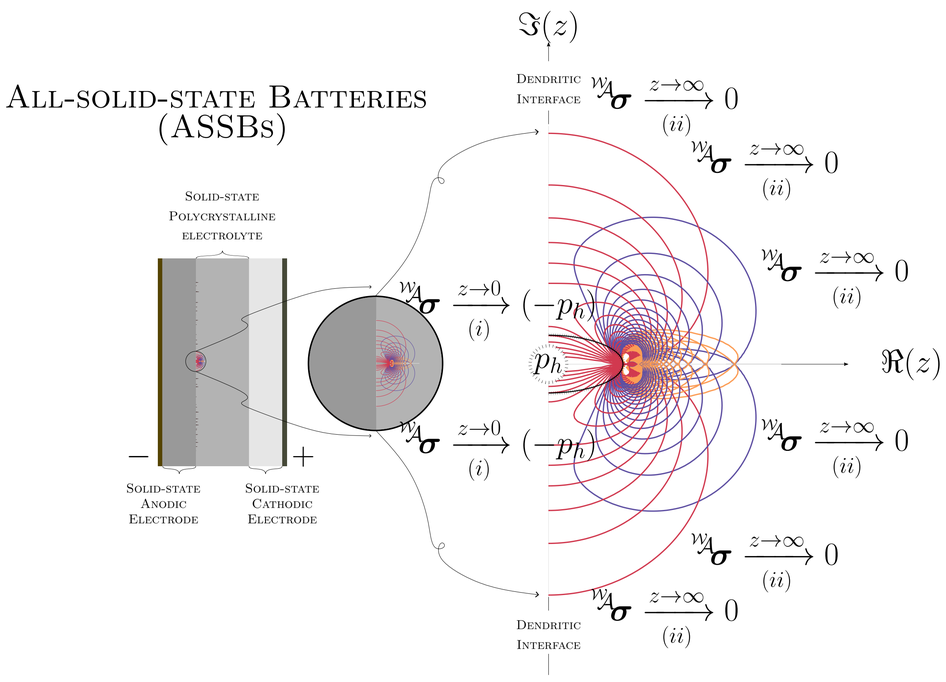

Interface Analysis

Interface between solid electrode and solid-state electrolyte (SE|SSE) taking place at space charge layer (SCL) [2] found in ASSBs critically exhibits mechanical and electrochemical instability [3]. This evidence points directly to the fact that the soft metallic li anode is erroneously prone to triggering dendrites, under cycles of electric charge & discharge [4].

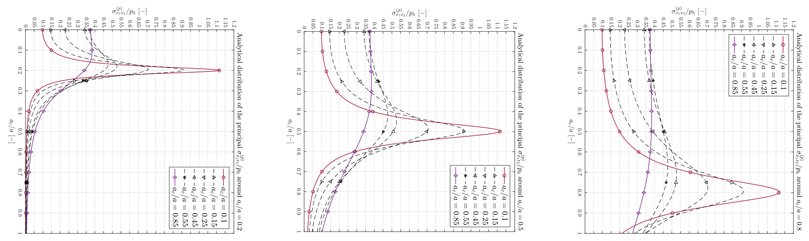

Distribution: ana. max. shear stress ${}^{w_{\mathcal{A}}}\sigma^{\Pi}_{x_1x_2}$ around crack tip a_c, where ${}^{w_{\mathcal{A}}}\sigma^{\Pi}_{x_1x_2}$ is based on Airy-Westergaard function defined by

$${}^{w_{\mathcal{A}}}\mathcal{A} : \mathbb{C}\to\mathbb{C}, z\mapsto {}^{w_{\mathcal{A}}}\mathcal{A}(z) := \Re\Big(\iint_\Gamma \mathcal{K}^{(\star)}\, dz\Big) + x_2\,\Im\Big(\oint_\Gamma \mathcal{K}^{(\star)}\, dz\Big),$$

$$\mathcal{K}^{(\star)} := \mathcal{K}^c : \mathbb{C}\to\mathbb{C}, z\mapsto \mathcal{K}^c(z) := -p_h + p_h/\sqrt{1-a^2/z^2},\ \forall\,\{p_h, a\}\in\mathbb{R}_+$$

Next-generation All-solid-state battery

Nucleation taking place at critical dendritic (SE|SSE)-interface

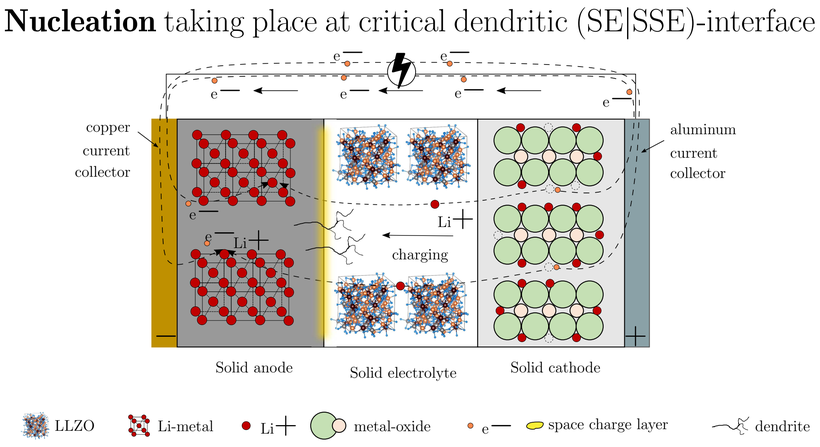

Thermodynamic consistency: satisfied.
Closure problem: fulfille by 15 moments.

Embedded structural-tensor SSE

Polycrystalline garnet-typed SSE such as LLZO exhibit a network of grain boundaries, and grains with various sizes and shapes under microscopic observation. Therefore, this type of microstructure is potentially prone to nuance destruction of ceramic-like materials.

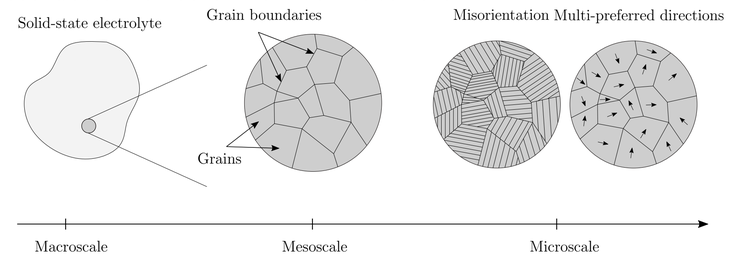

Consequentially, dendrites contribute to degradation of ionic conductivity and cracks via tracing along grain boundaries.

Nucleation interface: Taking place at the critical dendritic interface

Coupled fields: Displacement vector field and temperature scalar field

$$\boldsymbol{u} : \begin{cases}\Omega\times\mathbb{R}_+\to\mathbb{R}^3,\\ (\boldsymbol{x},t)\mapsto\boldsymbol{u}(\boldsymbol{x},t),\end{cases}\quad \theta : \begin{cases}\Omega\times\mathbb{R}_+\to\mathbb{R},\\ (\boldsymbol{x},t)\mapsto\theta(\boldsymbol{x},t),\end{cases}\quad \theta : \begin{cases}\Omega\times\mathbb{R}_+\to\mathbb{R},\\ (\boldsymbol{x},t)\mapsto\theta(\boldsymbol{x},t),\end{cases}$$

Governing conservation equations

$$\frac{d}{dt}\int_\Omega (\cdot)\, d\Omega = \int_\Omega (\cdot)^{\text{action}}\, d\Omega + \int_{\partial\Omega} (\cdot)^{\text{action}}\, d\partial\Omega + \int_\Omega (\cdot)^{\text{production/source/sink}}\, d\Omega$$

$\rho(\boldsymbol{x},t)$ is mass density per unit volume (puv); $\boldsymbol{b}(\boldsymbol{x},t)$ body force puv; $\boldsymbol{v}(\boldsymbol{x},t)$ velocity; $e(\boldsymbol{x},t)$ internal energy puv; $\boldsymbol{q}(\boldsymbol{x},t)$ heat flux; $r(\boldsymbol{x},t)$ heat source puv; $\boldsymbol{\sigma}$ Cauchy stress and $\boldsymbol{\varepsilon}$ infinitesimal strain. Helmholtz energy functional

$$a_{\text{Griffith}} := a^* = \arg\min_{a\in\mathbb{R}} \iiint_\Omega f(a, \boldsymbol{u}; \lambda, \mu, \boldsymbol{d}\otimes\boldsymbol{d})\, d\Omega - \iint_\Gamma f(a;\gamma)\, d\Gamma \Big|_{\boldsymbol{u}^{(s)}}$$

Governing PDE

$$a_{\text{Griffith}} := a^* = \arg\min_{a\in\mathbb{R}} \iiint_\Omega f(a, \boldsymbol{u}; \lambda, \mu, \boldsymbol{d}\otimes\boldsymbol{d})\, d\Omega - \iint_\Gamma f(a;\gamma)\, d\Gamma \Big|_{\boldsymbol{u}^{(s)}}$$

Strain energy: Interface between solid electrode and solid-state electrolyte (SE|SSE) taking place at space charge

$$\iiint_\Omega f(a, \boldsymbol{u}; \lambda, \mu, \boldsymbol{d}\otimes\boldsymbol{d})\, d\Omega$$

Surface energy: Interface between solid electrode and solid-state electrolyte (SE|SSE) taking place

$$\iint_\Gamma f(a;\gamma)\, d\Gamma$$

Therefore

$$\rho\,\partial^2_{t^2}\boldsymbol{u}^{(s)} + \nabla\cdot\Big(\overset{4}{\mathbb{C}}{}^{f^{\mathbb{D}(\Omega)}_{(\lambda,\mu)}} : \nabla\boldsymbol{u}^{(s)}\Big) + \rho\nabla V_e = \boldsymbol{0},$$

$$\text{s.t.}\quad a_{\text{Griffith}} := a^* = \arg\min_{a\in\mathbb{R}} \iiint_\Omega f(a, \boldsymbol{u}; \lambda, \mu, \boldsymbol{d}\otimes\boldsymbol{d})\, d\Omega - \iint_\Gamma f(a;\gamma)\, d\Gamma \Big|_{\boldsymbol{u}^{(s)}}$$

Boundary condition settings

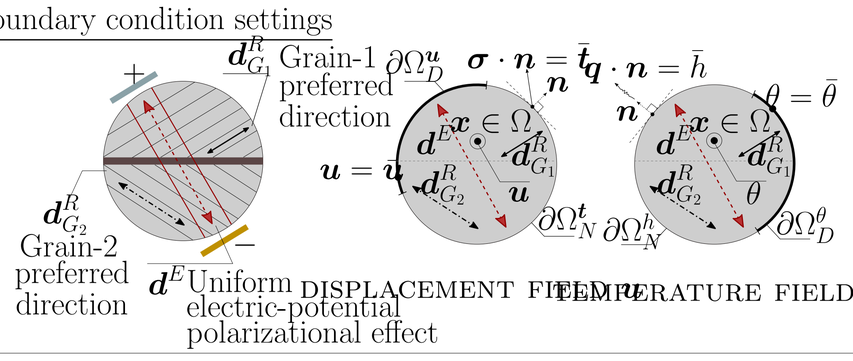

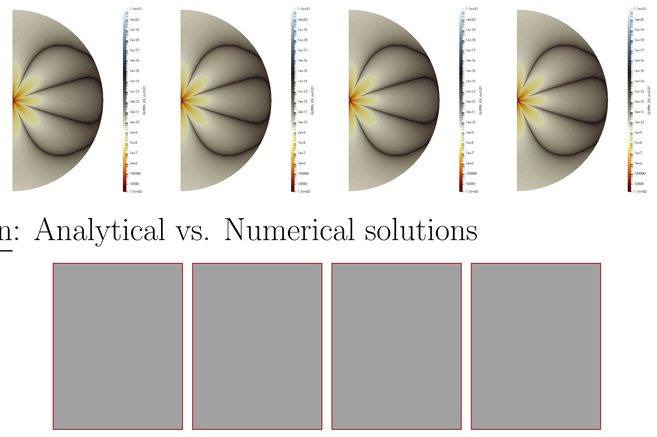

Comparison: Analytical vs. Numerical solutions

PDE

FEM implementation: Element stiffness matrix $\boldsymbol{K}^e$: known; approximated by Gauss quadrature rule; index notation implies $4+2$ *for*-loop:

$$K^{e\,\alpha\beta}_{ik} = \int_{\Omega^\xi}\Big(\mathcal{L}^\alpha_1\,\mathbb{C}^{f^{GL}}_{i1k1}(y)\,\mathcal{R}^\beta_1 + \mathcal{L}^\alpha_1\,\mathbb{C}^{f^{GL}}_{i1k2}(y)\,\mathcal{R}^\beta_2 + \mathcal{L}^\alpha_2\,\mathbb{C}^{f^{GL}}_{i2k1}(y)\,\mathcal{R}^\beta_1 + \mathcal{L}^\alpha_2\,\mathbb{C}^{f^{GL}}_{i2k2}(y)\,\mathcal{R}^\beta_2\Big)\det(\boldsymbol{J})\, d\Omega^\xi$$

where $\mathcal{L}^\alpha_j$ and $\mathcal{R}^\beta_l$ are gradients of basis functions at node α^{th} and β^{th}, respectively.

Contact

Tuan Vo
vo@acom.rwth-aachen.de

References

[1] **T.Vo**, *Modeling the swelling phenomena of li-ion batt. cells based on a numerical chemo-mech. coupled approach.* MA, Robert Bosch Battery Systems GmbH, 2018.

[2] **S.Braun**, C.Yada and A.Latz, *Thermodynamically consistent model for Space-Charge-Layer formation in a solid electrolyte.* Jr. Phys. Chem., 119, 22281-22288, 2015.

[3] **C.Hüter**, S.Fu, M.Finsterbusch, E.Figgemeier, L.Wells, and R.Spatschek, *Electrode-electrolyte interface stability in solid state electrolyte system: influence of coating thickness under varying residual stresses.* AIMS Materials Science, 4(4):867-877, 2017.

[4] **S.Kim**, J.S.Kim, J.Miara, Y.Wang, S.K.Jung, S.Y.Park, Z.Song, H.King, M.Badding, J.M.Chang, V.Roev, G.Yoon, B.Kim, J.H.Kim, K.Yoon, D.Im, and K.Kang,